Volume 16 | Number 15 | 21 April 2014 | Pages 3049–3236

CrystEngComm

www.rsc.org/crystengcomm

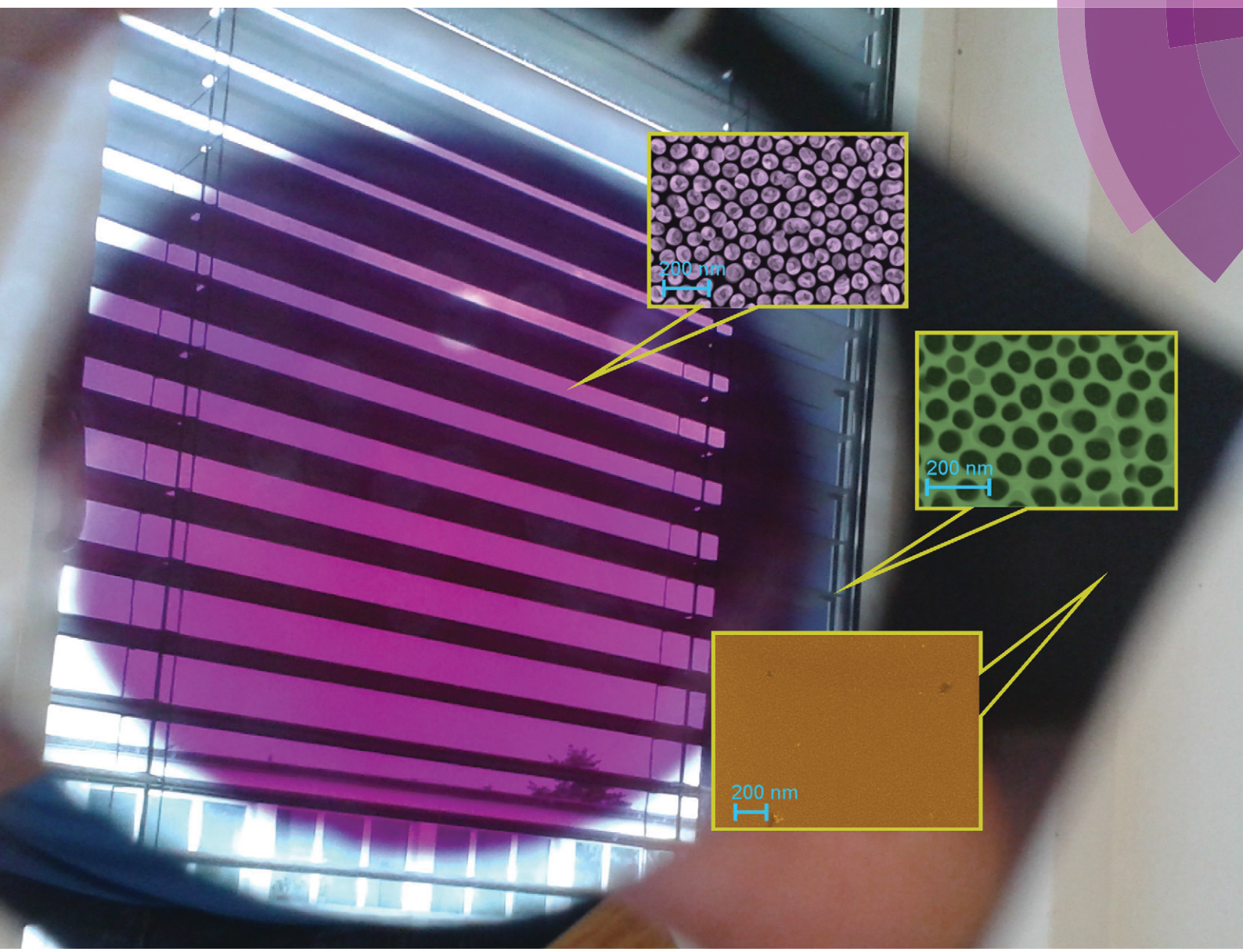

ROYAL SOCIETY OF CHEMISTRY

COVER ARTICLE

Habouti and Es-Souni

Au-NR/VO_2-NP nanocomposites supported on glass substrates: microstructure and optical properties

CrystEngComm

COMMUNICATION

View Article Online
View Journal | View Issue

Cite this: *CrystEngComm*, 2014, **16**, 3068

Received 16th October 2013,
Accepted 6th January 2014

DOI: 10.1039/c3ce42097c

www.rsc.org/crystengcomm

Au-NR/VO_2-NP nanocomposites supported on glass substrates: microstructure and optical properties†

Salah Habouti and Mohammed Es-Souni*

On-glass-substrate gold nanorods (Au-NRs) are processed *via* electrodeposition into anodized alumina template films that were fabricated using an Al/Au/Ti film stack on glass. The Au-NRs are capped with VO_2 nanoparticles obtained from sputtered vanadium caps. The nanostructure arrays show intense plasmon resonance and are thermochromic with VO_2 size dependent transition temperature.

Composites of oxide nanoparticles (NPs), mostly semiconductor oxides and noble metal nanostructures, are the focus of intense research activities because they show promising light harvesting properties for applications spanning the range from dye sensitized solar cells, to water splitting, to photocatalysis.[1,2] The improved light absorption in the main solar spectrum range of these nanocomposites – that is at the origin of their superior properties – is mediated by the localized surface plasmon resonance of the noble metal nanoparticles.[1,2] However, with the exception of the recent work by the group of Moskovits,[2] where supported Au-nanorods were used as a plasmonic substrate, research is mostly focused on colloidal NPs and films limiting practical use in the case of the former and available active surface for the latter.

Supported discrete nanocomposites are most propitious to control both surface area and structure dimensions which in turn allow the tuning and control of the absorption range.

In the present paper, we report on the fabrication of supported Au-nanorods (NRs) using thin porous alumina films (PAF) on glass substrates that were subsequently capped with VO_2-NPs. These nanocomposites present unusual optical properties as they combine plasmonic absorption with thermochromism. Reports on on-substrate 1D noble metal nanostructures using supported PAF are scarce,[4] among them our own work,[5] and a recent study on supported Au-NR/TiO_2 nanocomposites for water splitting.[2] Notwithstanding their somewhat laborious processing, supported plasmonic structures have substantial advantages over nanostructures processed *via* freestanding PA membranes, because they are easy to handle and can be better scaled-up for device applications as a variety of substrates, including technologically important ones such as ITO glass and polymers, may be used.

The experimental procedure is described in detail in the ESI and Fig. 1s† schematically describes the fabrication steps of the AAO films and Au-NR electrodeposition.

SEM micrographs of the PAF template as well as the Au-NR array are shown in Fig. 1. The electrolyte used here leads to corrugated NRs with furrow-like appearance. Their distribution is homogeneous (see Fig. 2s†) with a mean spacing of 50 nm, a mean diameter of 70 nm and a mean length of 300 nm.

The extinction spectrum of these NRs is also displayed in Fig. 1 and shows a sharp and intense absorption maximum at 540 nm and a broad weak absorption peak centred around 900 nm. These peaks arise from the anisotropy of the Au-NRs that lead to the splitting of dipole plasmon resonance into transverse (540 nm) and longitudinal (900 nm) modes.[5,6] Their loci are known to be dependent on dimensions (diameter and length), spacing and dielectric environment of the NRs.[6]

Fig. 2a shows the Au-NRs after sputtering 10 nm of elemental vanadium. The vanadium layer condenses primarily on the NR tips forming caps (5 nm V on NRs could not be resolved). The nature of the interface between Au and V is not known, but the Au–V phase diagram,[7] both in the V- and in the Au-rich region, shows the formation of solid solutions with eventually the presence of intermetallic phases depending on composition and temperature. Hence, we may expect intermixing between V and Au at the interface at least for a few atomic layers upon sputtering. After heat treatment (Fig. 2b and c), VO_2 (see below for phase analysis) grows on top of the Au-NRs and either forms NPs (in the case of

Institute for Materials & Surface Technology (IMST), 24149 UAP Kiel, Germany. E-mail: me@fh-kiel.de; Fax: +49 431 210 2660; Tel: +49 431 210 2660

† Electronic supplementary information (ESI) available: Materials and methods: processing of PAF template films on glass substrates; processing of Au-NRs and VO_2 capped Au-NRs; characterization methods; Fig. 1s–5s. See DOI: 10.1039/c3ce42097c

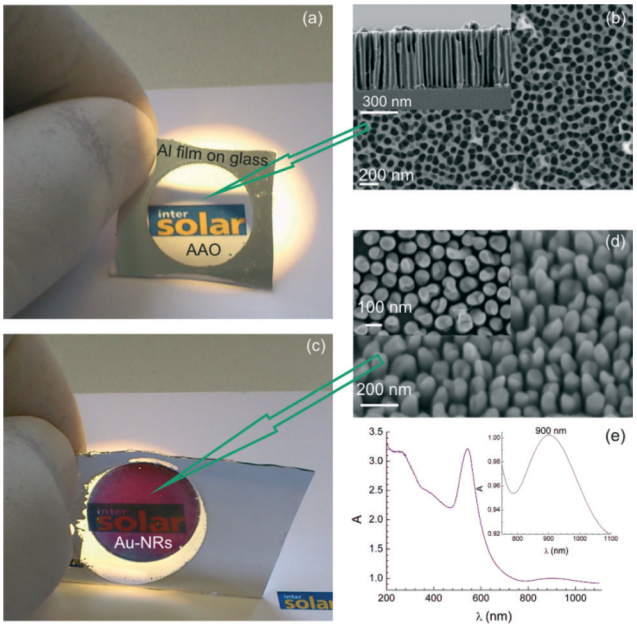

Fig. 1 (a) Photograph showing the transparent PAF on glass (surrounding it is the non-anodized Al-film); (b) SEM micrograph of the PAF template, top view and cross-section (inset); (c) photograph of the electrodeposited Au-NR after removal of PAF; (d) SEM micrograph of the Au-NRs: tilted and top (inset) views; (e) UV-Vis optical absorption properties showing two plasmonic peaks (see text for discussion).

5 nm V) (Fig. 2b (see also Fig. 2s†)) or grows vertically, forming NRs consisting of stacks of nanosheets that are well visible in Fig. 2c. Some of the VO_2 nanostructures in Fig. 2c merge laterally but the majority of them grow vertically, forming discrete structures on the Au-NRs.

Structural analysis using XRD was not conclusive as only very weak and broad peaks of VO_2 could be obtained from grazing incidence patterns of the 10 nm film (V thickness) (Fig. 3s†). In contrast, Raman scattering demonstrates unambiguously the presence of characteristic vibrations of VO_2 that are very well resolved down to 5 nm (vanadium thickness) (Fig. 3) even at the lowest laser power of 0.2 mW that is necessary in order to prevent oxidation of VO_2 to V_2O_5 during measurement.

The observation of tiny amounts of VO_2@Au-NRs using Raman scattering with the relatively high band intensities shown in Fig. 3 is a direct consequence of surface enhanced Raman scattering (SERS) that is a very well-known method for the analysis of trace amounts of different substances, and is based on electromagnetic field enhancement by the plasmonic structure.[9] Most of the published studies, however, are on dyes and other organic molecules, including DNA, as well as viruses.[10] The only work on SERS of oxides is by Donev *et al.* who reported on Au-capped VO_2 particles of 120 nm that were fabricated by pulsed laser deposition and lithographic techniques (in their work, Au was placed on VO_2).[3]

The present study shows that supported Au-NRs may constitute powerful substrates for the detection of inorganic NPs, in addition to their high enhancement factor shown in

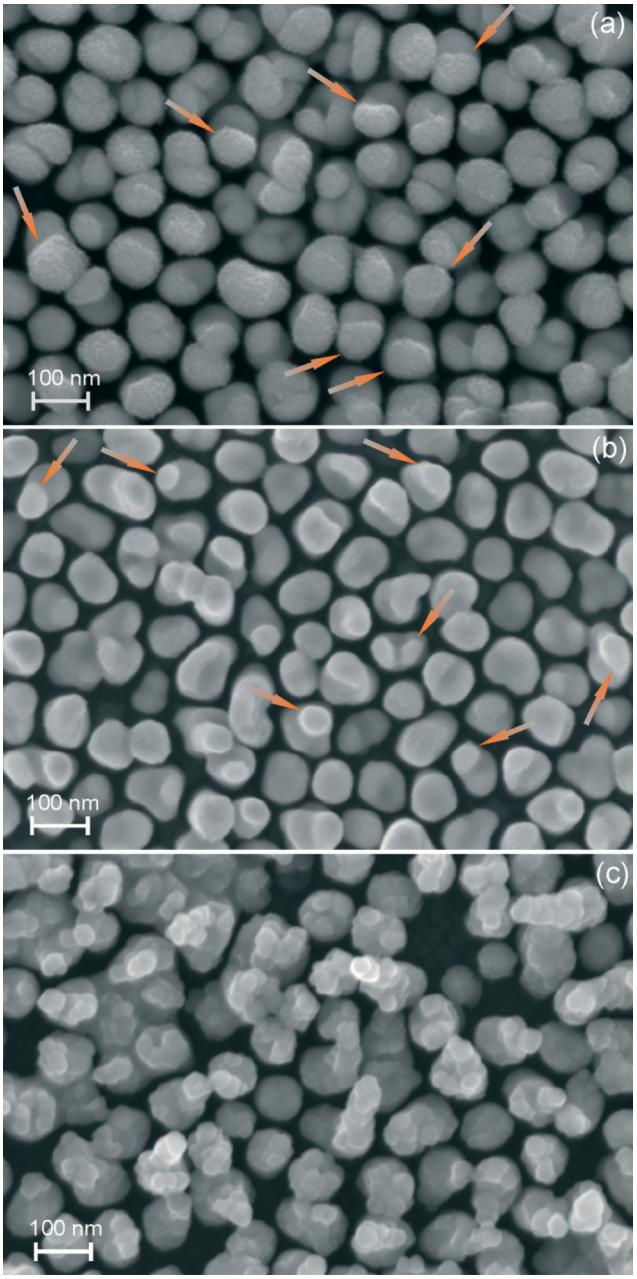

Fig. 2 (a) SEM micrograph of vanadium capped Au-NRs obtained by sputter deposition of 10 nm vanadium. The caps are clearly seen on top of the Au-NRs (arrows); (b) SEM micrograph of VO_2-NPs (arrows) on top of Au-NRs obtained after annealing 5 nm sputtered vanadium; (c) VO_2-NPs and NRs obtained from 10 nm sputtered vanadium and growing vertically on Au-NRs.

earlier work for organic molecules.[5] Moreover, as mentioned above, they can also be advantageously used as an active support for other functional nanomaterials, among them VO_2 that constitutes a highly interesting multifunctional material. VO_2 is a well-known thermochromic material that undergoes a reversible semiconductor–metal phase transition (SMT) at 68 °C from a low temperature monoclinic ($P2_1/c$) to a metallic tetragonal phase ($P4_2/mnm$) with a rutile structure (VO_2 (R)).[11] The metallic phase exhibits high reflectance in the IR range

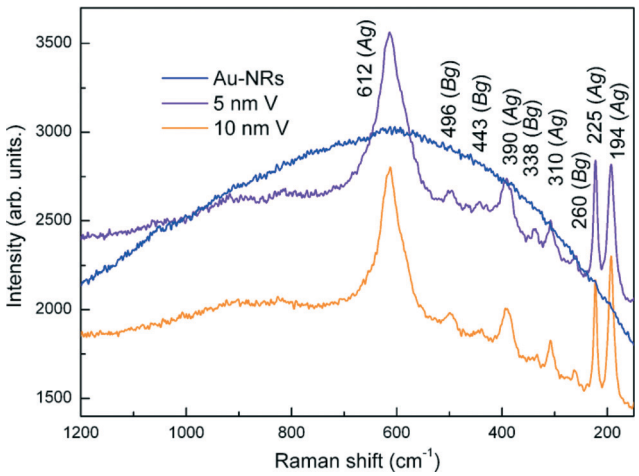

Fig. 3 Raman scattering spectra showing the characteristic vibrations of VO_2 (ref. 8) obtained from VO_2-NPs on Au-NRs corresponding to Fig. 2b and c. The VO_2-NPs were obtained after annealing 5 and 10 nm of sputtered vanadium on Au-NRs. The fluorescence spectrum of the Au-NRs is also shown.

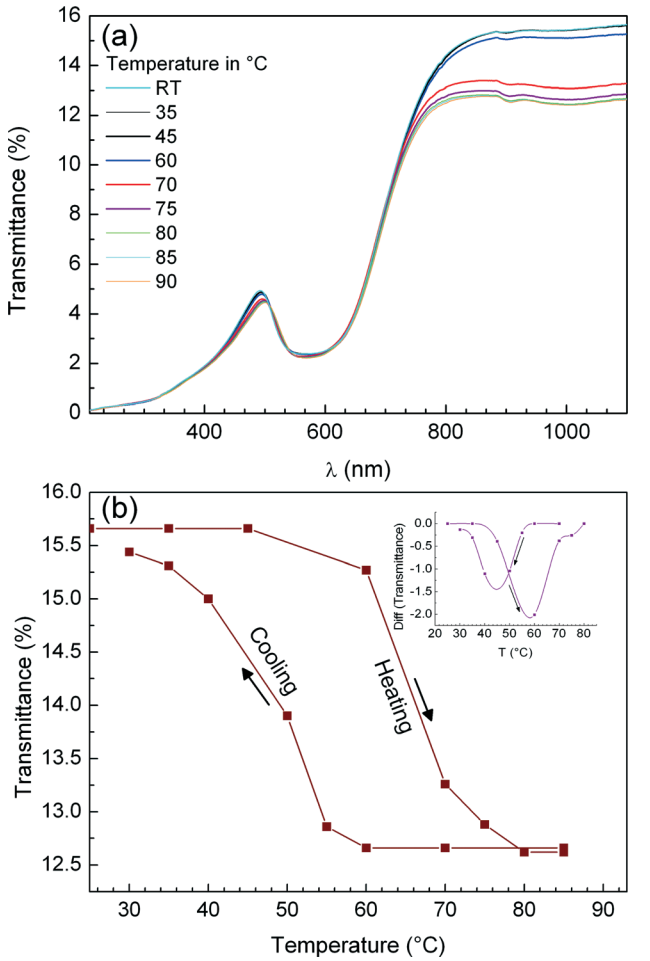

Fig. 4 (a) UV-Vis transmission spectra of VO_2-NPs@Au-NRs at different temperatures. The transmission minimum corresponds to the transverse plasmonic mode of Au-NRs in the presence of VO_2 NPs. The decrease in transmittance in the near IR region results from the semiconductor–metal transition of VO_2. (b) Forward and backward transmittance as a function of temperature at a wavelength of 1100 nm for 10 nm VO_2 on Au-NRs. The inset shows the derivative of the hysteresis loop to determine the phase transition temperature.

without trade-off of transmittance in the visible region that makes VO_2 promising for smart window applications. The main benefit lies in minimizing energy consumption for air conditioning of buildings without all too strongly impairing visible light transmission.[12] However, one serious hindrance for industrial application is the high transition temperature which, for higher efficiency, must be lowered to below 40 °C. Doping with Mo and W was shown to decrease the SMT temperature in discrete nanostructures to room temperature, depending on doping concentration (see the review by Whittaker *et al.*[13]). Scaling VO_2 down to nanosize dimensions can also affect the SMT characteristics, with the transition temperature being strongly correlated to clamping and stress effects from the substrate.

The UV-Vis-transmittance properties of the VO_2@Au-NR structure at different temperatures are shown in Fig. 4a. The minimum at 540 nm for the bare Au-NRs is red-shifted to 565 nm for VO_2-NPs@Au-NRs that can be explained by the different dielectric environments arising from the presence of VO_2, a well-known effect on plasmonic structures.[14] At the onset of SMT at 60 °C (see below), a small red-shift of 4 to 6 nm is also observed due to the structural change. The weak longitudinal plasmonic peak at 900 nm is strongly attenuated by the presence of VO_2-NPs. With increasing temperature, the transmittance decreases in the near IR region and substantially between 60 and 70 °C, owing to SMT. This behaviour is reversible with the formation of a hysteresis (Fig. 4b), characteristic for this type of martensitic transformation, because the reversible phase transformation is limited by nucleation and growth. The VO_2-NPs derived from the 10 nm thick vanadium film show a somewhat broad hysteresis loop with a forward transformation temperature of approximately 60 °C and a backward temperature of 45 °C. In contrast, a shallower hysteresis loop is obtained from the 5 nm thick vanadium film with transformation temperatures of approximately 45 and 40 °C for the forward and backward transformation, respectively (Fig. 4s†).

The values obtained for the SMT temperature largely differ from that of bulk VO_2. This might be regarded as the consequence of two correlated effects: the nanoscale dimension of the VO_2-particles and the electron injection from the Au-NRs. The VO_2–Au interface is a semiconductor–metal heterojunction involving different work functions (5.4 eV for VO_2 (ref. 15) and 4.8 eV for Au with respect to the vacuum level). Electrons are expected to flow through the junction from Au leading to band-bending (valence and conduction band) of VO_2 toward the metal junction and alignment of the Fermi levels. This is schematically depicted in Fig. 5s.† It is thought that the increase of electron concentration in the semiconducting phase leads to its destabilization, thus lowering the energy barrier of the transformation into the metallic phase. This mechanism is rather in favor of the Mott–Hubbard

transition,[11] already put forward for the lowering of the SMT temperature in epitaxial VO_2 thin films covered with Au-NPs.[16] The occurrence of plasmon electrons is a prerequisite for lowering the SMT transition temperature, as we have shown in previous work that the presence of VO_2 on large Au-clusters did not result in any SMT shift.[17]

The 5 nm vanadium film yields mostly single VO_2-nanoplatelets of 20 to 50 nm diameter on top of the Au-NRs, and may explain the lower SMT temperature obtained here. In contrast, the 10 nm film results in larger VO_2 structures that are made of VO_2 nanoplatelet stacks, as mentioned above and shown in Fig. 2c. In this case, the effect of the Au–VO_2 interface on the SMT temperature is thought to be mitigated by the more sluggish transformation away from the interface, *i.e.* along the platelet stack. There are, however, additional effects that should also contribute to the lowering of the SMT temperature. For instance, interfacial stresses and stresses arising from SMT that could hinder phase transformation might be considered minimal because the VO_2-NPs are supported on self-standing Au-NRs that imply low hydrostatic stresses, provided that nucleation and growth are from surface sites.[13]

In summary, a novel on-glass-substrate supported nanostructure array consisting of VO_2 capped Au-NRs was presented. The processing method can be extended to other noble metals and functional oxide nanostructures and is easily scalable to larger area structures. The particular structure reported here combines localized surface plasmon resonance through Au-NRs and thermochromic properties *via* VO_2-NPs. The thermochromic properties of the structure, demonstrated *via* temperature dependent transmission measurements, are largely size dependent with a semiconductor–metal transition temperature of roughly 40 °C for VO_2-NPs in the size range from 20 to 50 nm.

Notes and references

1 Y. Tian and T. Tatsuma, *J. Am. Chem. Soc.*, 2005, **127**, 7632–7637; Y. Nishijima, K. Ueno, Y. Yokota, K. Murakoshi and H. Misawa, *J. Phys. Chem. Lett.*, 2010, **1**, 2031; A. Tanaka, S. Sakaguchi, K. Hashimoto and H. Kominami, *ACS Catal.*, 2013, **3**, 79.
2 J. Lee, S. Mubeen, X. Ji, G. D. Stucky and M. Moskovits, *Nano Lett.*, 2012, **12**, 5014–5019; S. Mubeen, J. Lee, N. Singh, S. Krämer, G. D. Stucky and M. Moskovits, *Nat. Nanotechnol.*, 2013, **8**, 247.
3 E. U. Donev, J. I. Ziegler, R. F. Haglund Jr. and L. C. Feldman, *J. Opt. A: Pure Appl. Opt.*, 2009, **11**, 125002.
4 G. A. Wurtz, P. R. Evans, W. Hendren, R. Atkinson, W. Dickson, R. J. Pollard and A. V. Zayats, *Nano Lett.*, 2007, **7**, 1297; S. Mátéfi-Tempfli and M. Mátéfi-Tempfli, *Adv. Mater.*, 2009, **2**, 4005.
5 S. Habouti, M. Mátéfi-Tempfli, C.-H. Solterbeck, M. Es-Souni, S. Mátéfi-Tempfli and M. Es-Souni, *Nano Today*, 2011, **6**, 12; S. Habouti, M. Mátéfi-Tempfli, C.-H. Solterbeck, M. Es-Souni, S. Mátéfi-Tempfli and M. Es-Souni, *J. Mater. Chem.*, 2011, **21**, 6269.
6 S. Link, M. B. Mohamed and M. A. El-Sayed, *J. Phys. Chem. B*, 1999, **103**, 3073; J.-W. Kim, E. I. Galanzha, V. Shashkov, H.-M. Moon and V. P. Zharov, *Nat. Nanotechnol.*, 2009, **4**, 688.
7 J. F. Smith, *Bull. Alloy Phase Diagrams*, 1981, **2**, 344.
8 P. Schilbe, *Phys. B*, 2002, **316**, 600.
9 S. Lal, N. K. Grady, J. Kundu, C. S. Levin, J. B. Lassiter and N. J. Halas, *Chem. Soc. Rev.*, 2008, **37**, 898.
10 J. Kneipp, H. Kneipp and K. Kneipp, *Chem. Soc. Rev.*, 2008, **37**, 1052.
11 A. Zylberstejn and N. F. Mott, *Phys. Rev. B: Solid State*, 1975, **11**, 4383.
12 Z. Zhang, Y. Gao, H. Luo, L. Kang, Z. Chen, J. Du, M. Kanehira, Y. Zhang and Z. L. Wang, *Energy Environ. Sci.*, 2011, **4**, 4290.
13 L. Whittaker, C. J. Patridge and S. Banerjee, *J. Phys. Chem. Lett.*, 2011, **2**, 745.
14 K. M. Mayer and J. H. Hafner, *Chem. Rev.*, 2011, **111**, 3828.
15 A. I. Gavrilyuk, T. G. Lanskaya, A. A. Mansurov and F. A. Chudnovskii, *Sov. Phys. Solid State*, 1984, **26**, 117.
16 G. Xu, C.-M. Huang, M. Tasawa, P. Jin, D.-M. Chen and L. Miao, *Appl. Phys. Lett.*, 2008, **93**, 61911.
17 R. Minch and M. Es-Souni, *CrystEngComm*, 2013, **15**, 6645.